

Basic Difference Between Brain and Computer: Integration of Asynchronous Processes Implemented as Hardware Model of the Retina

Andrzej W. Przybyszewski, Paul S. Linsay, Paolo Gaudiano, and Christopher M. Wilson

Abstract—There exists a common view that the brain acts like a Turing machine: The machine reads information from an infinite tape (sensory data) and, on the basis of the machine's state and information from the tape, an action (decision) is made. The main problem with this model lies in how to synchronize a large number of tapes in an adaptive way so that the machine is able to accomplish tasks such as object classification. We propose that such mechanisms exist already in the eye. A popular view is that the retina, typically associated with high gain and adaptation for light processing, is actually performing local preprocessing by means of its center-surround receptive field. We would like to show another property of the retina: The ability to integrate many independent processes. We believe that this integration is implemented by synchronization of neuronal oscillations. In this paper, we present a model of the retina consisting of a series of coupled oscillators which can synchronize on several scales. Synchronization is an analog process which is converted into a digital spike train in the output of the retina. We have developed a hardware implementation of this model, which enables us to carry out rapid simulation of multineuron oscillatory dynamics. We show that the properties of the spike trains in our model are similar to those found *in vivo* in the cat retina.

Index Terms—Brain computation, quasi-periodic oscillations, synchronization, universal Turing machine, visual system.

I. INTRODUCTION

THERE is an extensive literature describing the similarities between the functioning of neural connections in the brain and an algorithmic machine (e.g., [1]–[3]). However, a different view is presented in several papers that the brain may not be performing computations in the sense of the universal Turing machine (e.g., [4]–[6]). In the following two examples, we will introduce some differences between the brain and a Turing machine. In this work we have modeled a small, autonomous part

of the brain, namely, the retina. We will describe processes related to retinal computation in relationship to two of its properties: maintained neural activity and synchronization. In the first case (maintained neural activity), if we consider the brain as a Turing machine, maintained network activity in the retina may give different results for repeated computation of the same input. This seems counterintuitive when compared with the results obtained on digital computers, however, notice that the definition of a Turing machine states that action is determined by input and internal state. Because the latter is constantly changing in the brain, the same inputs can give rise to different activations. In the second case (synchronization), it is well known that different parallel pathways in the retina operate with different speeds, as shown for example in the pathways that originate with type X and type Y retinal ganglion cells. Also, it is known that different levels of light adaptation significantly change delay and speed of retinal processing. This would indicate that information coming from different parallel pathways is not synchronized, which may result in a discrepancy in the results of neural computation across pathways as the speed of the various pathways changes. These discrepancies can be observed on several time scales by synchronizing these processes in different time periods.

Unlike digital computers, where a central clock paces each calculation with a single-bit precision, brain neurons show variable, only partly synchronized patterns of the single-bit spike trains. In addition to the information carried in spike trains, it is likely that additional information is carried in the so-called “maintained neural activity.”

A common practice in studies of neural activity is to remove all variability and assume that significant information carried by neural signals is synchronized with the input (stimulus). Typically, the same experiments are repeated many times and the cell's responses are averaged across multiple readings. This approach assumes that the information in the spike trains consists of two main components: 1) a signal, presumed to be the invariant part of the spike train, which is constant for the same input; and 2) noise, the variable part of the spike train, which results from many different processes related to the maintenance of the brain independent of the actual sensory input. Response averaging removes noise and extracts signal under the assumption that the signal always stays in the same phase related to the input. However, recent experiments [7] show that neurons in the visual cortex show synchronized oscillations in response to relevant stimuli which are not always phase-locked to the stimulus and would go unnoticed in averaged responses of a single

Manuscript received September 5, 2005; revised May 23, 2006.

A. W. Przybyszewski was with the Department of Cognitive and Neural Systems, Boston University, Boston, MA 02215 USA. He is now with the Department of Neurology, University of Massachusetts Medical Center, Worcester, MA 01655 USA and with the Department of Psychology, McGill University, Montreal, QC H3A 1B1, Canada (e-mail: przy@ego.psych.mcgill.ca).

P. S. Linsay was with the Plasma Fusion Center, Massachusetts Institute of Technology (MIT), Cambridge, MA 02139 USA. He is now with Linsay Associates, Newton, MA 02458 USA.

P. Gaudiano was with the Department of Cognitive and Neural Systems, Boston University, Boston, MA 02215 USA. He is now with the Icosystem Corporation, Cambridge, MA 02138 USA.

C. M. Wilson was with Massachusetts Institute of Technology (MIT), Cambridge, MA 02139 USA. He is now with the Chalmers University of Technology, Goetheborg SE-412 96, Sweden.

Color versions of one or more of the figures in this paper are available online at <http://ieeexplore.ieee.org>.

Digital Object Identifier 10.1109/TNN.2006.882814

neuron [7]. These oscillations can be seen in the integrated activity of many neurons, in what is referred to as *local field potential*. If these integrations are performed along neurons extracting certain input (stimulus) attributes, they may encode figure-background separation in the higher visual areas [7]–[10], [107].

The purpose of this study is to show that already in the retina such oscillatory processes exist, and that they extract certain attributes of the stimulus. Therefore, we hypothesize that the purpose of retinal processing is not only to perform gain control, adaptation, and center-surround receptive processing, but also to integrate many processes related to properties of the inputs. This manifests itself as oscillations observed in the local field electroretinogram (ERG) [11] or in ganglion cell membrane potential [11], [12].

In order to check this hypothesis, we have assumed, on the basis of electrophysiological experiments (see Section I-A), that in the retina there are at least three assemblies of networks/neurons showing oscillations in different ranges of frequencies. There is also more direct experimental evidence that the intracellular generator potential in retinal ganglion cells, which is a membrane potential without spikes [9], shows oscillations that are not necessarily phase-locked to the light stimulus [13]. By changing stimulus attributes, the generator potential oscillations could be changed from locked to the input to nonlocked, and vice versa. In contrast, nonoscillatory components of the ganglion cell responses are always locked to the stimulus [13].

Our approach is not completely new. Wilson and Cowan [14] proposed that the central nervous system can be divided into inhibitory and excitatory oscillating populations with mutual coupling between them. This theory was later applied by Freeman and others to specific parts of the brain such as the olfactory system [15]–[17], [106], and compared to electroencephalograms (EEG) signals in animals [16]. Baird [11] used a similar model to construct a unified theory of pattern recognition and associative memory. However, theoretical (analytical) analysis of the behavior of coupled nonlinear oscillators even for small numbers of oscillators is difficult [18]–[20]. Also, typically nonlinear oscillators exhibit quasi-periodic or chaotic behavior, which looks similar to the noise observed in experimental recordings.

A. Experimental Evidence of Different Oscillatory Processes in the Retina

As early as in 1928, Adrian and Matthews [21] reported that illumination of a large portion of the retina induced a rhythmic discharges. They suggested that the oscillations were evoked by the lateral summation of multiple inputs. Since this initial observation, retinal oscillations have been observed in many laboratories [21]–[26]. It has been found that the frequency and duration of the retinal oscillations can be affected by light intensity [11], [21], rate of stimulation [21], and application of drugs or anaesthetics [11], [21], [24], [25], [27]. It has been suggested that the retinal oscillatory potentials are postsynaptic in origin and are generated by reverberating interaction of ganglion, amacrine, and interplexiform cells in the inner retina [28]–[34]. The physiological interpretation of these oscillators is as follows.

The slowest oscillator, with frequencies around 6 Hz, may be associated with the horizontal cell network [35]–[37]: In response to sinusoidal gratings at photopic luminance level, the temporal transfer function of horizontal cells exhibits bandpass characteristics ranging from 3 to 10 Hz with a maximum response amplitude of 3–6 Hz [36].

A faster oscillator, with frequencies around 45 Hz, may be related to amacrine cells. Narrow-field bistratified (NFB) amacrine cells have been shown to respond to light with 50-Hz oscillatory potentials [38]. NFB amacrine cells are in the rod pathway in the rabbit retina. The origin of their oscillatory responses is unclear, but these oscillations appear to sharpen the transient on-response of the amacrine cells in comparison to the response of the rod bipolar cells [38]. Sakai and Naka [39] have recorded simultaneously from N-ON (NA) and N-OFF (NB) amacrine cells in the catfish retina. In these cells, the power spectra of the membrane noise in the dark or during steady illumination often showed a peak at 35 Hz. Such membrane noise is synchronized in phase among NA and NB cells, and is out of phase between NA and NB cells in the dark [39]. Similar synchronized oscillations were recently observed in AII cells in the mammalian retina [40].

Even faster oscillations, with frequencies around 140 Hz may be related to the push-pull effect of ON-OFF bipolar cells [41]. Experimental studies of the vertebrate retina, including the primate, have shown that oscillatory potentials of the ERG are in the range of 140 Hz [41]. The oscillatory potentials are probably generated by bipolar cells [24], [30], [31] based on the following evidence: 1) oscillatory potentials, like bipolar cells, extend over a substantial retinal depth [34]; 2) bipolar cells receive both rod and cone inputs, and oscillatory potentials show interaction between photopic and scotopic inputs [42], [43]; and 3) bipolar cells are segregated into ON and OFF channels similarly to oscillatory potentials [44]. We have found oscillations in the range from several hertz to about 150 Hz in the intracellular (generator) potentials of cat ganglion cells [13]. Frequencies in the range 20–120 Hz were observed in the ganglion cell spike trains [12], [26], [45].

B. Variability of Interspike Intervals and Noise

In the retina, spikes are generated almost exclusively in the ganglion cells. Therefore, analog interactions between activities of most retinal cells could be more sensitive to noise than interactions between spiking cells. However, interactions between nonspiking cells could be also a source of many different oscillations in the intracellular potential of the ganglion cell. There are many sources of noise in the retina such as the quantal nature of light, fluctuations in membrane conductances, or quantal nature of synaptic transmission. However, it is not clear how much noise is in the ganglion spike trains.

Some theoretical research suggests that noisy systems of coupled oscillators can produce a regular output. On the macroscopic level, a system of globally coupled oscillators may show low-dimensional dynamics, while microscopic variables follow high-dimensional chaos [46]–[49]. For example, Kaneko *et al.* [47] showed that by adding noise to the microscopic level of a system of globally coupled maps, their macroscopic behavior changed from high-dimensional chaos to low-dimensional

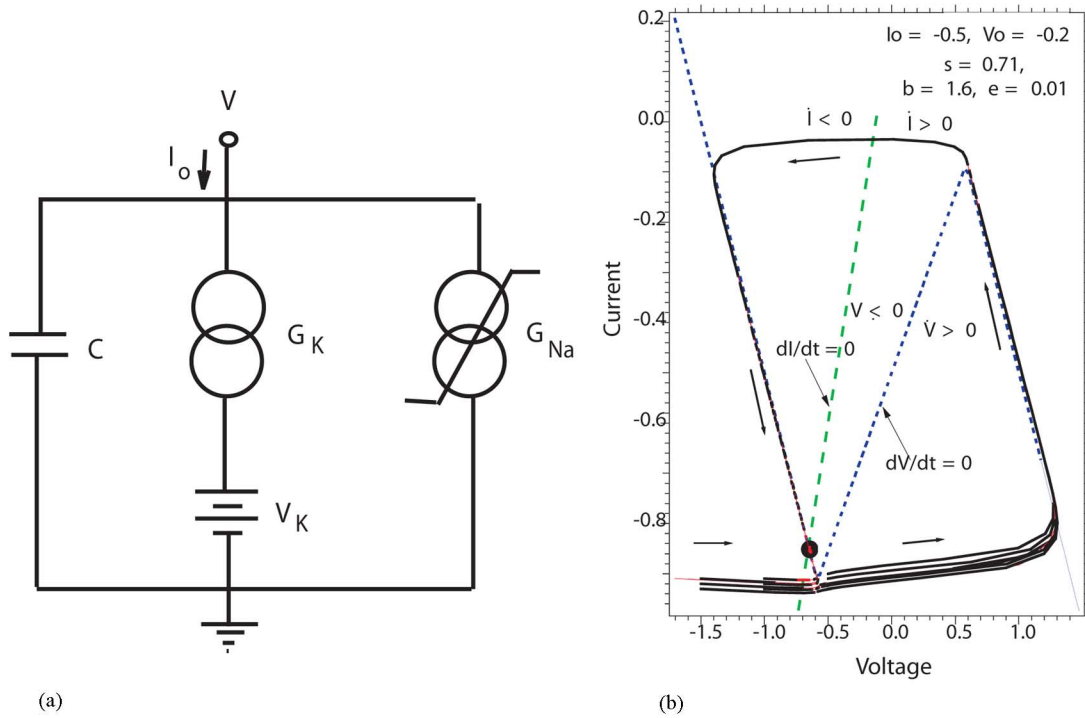


Fig. 1. (a) Electrical equivalent circuit model of a two-channel neuron: C —membrane capacitance, G_K —conductance of the potassium channel, V_K —equilibrium potassium potential, and G_{Na} —conductance of the sodium channel; (b) Oscillations of the Keener circuit with a large nonlinearity $\epsilon = 0.01$: Phase plot of current versus voltage. The equilibrium point is determined by the crossing the nullclines, as described in Section II-A. The unstable equilibrium point is marked with a dot.

noiseless motion. In addition, recent experiments [50], [51] have shown that in response to a large class of rapidly varying stimuli, retinal ganglion cell exhibited reproducible spike trains. If the stimulus is repeated, the clusters of spikes occur reliably at the same times, sometimes to within 1 ms. Similarly, in other sensory systems like in the trigeminal system of the rat, whisker deflections produce spikes which occur at precisely the same time in each trial [52].

In this paper, we compare properties of the experimental spike trains from the cat retina [13] with the train of pulses generated by a system of coupled nonlinear oscillators. We present a network of seven ganglion cells (G -neurons) built in agreement with anatomical and physiological retinal properties. We built this simulated network in hardware as coupled nonlinear oscillators.

There are several reasons for using electronic hardware to simulate retinal processing. The primary reason is the ability to scale the network size. In general, numerical integration becomes more costly as the number of neurons and neuronal connections increases. In contrast, increasing the number of neurons or connections in a hardware circuit may require additional time for construction of the circuit, but once the circuit is built, the speed of simulations is independent of the network size or connectivity. In fact, our hardware circuit (as described in Section II-B) was actually scaled to run at a speed significantly higher than that of retinal cells. This makes it possible to run a vast number of simulations, much more readily than could possibly be done in software even on the fastest computers. Hence, a hardware model of the retina makes it possible to analyze long spike trains in stable conditions and to explore additional

regions of the potentially infinite space of stimulus amplitude and frequency combinations. This flexibility has the potential to yield new perspectives on retinal dynamics. We were especially interested in differentiating regions of the input space where oscillations were locked or unlocked to the input.

Another interesting aspect of using hardware for simulation of retinal cells is that our model, just like retinal cells, is noisy. Circuits were not thermally stabilized, which gives rise to endogenous sources of noise, not unlike the noise that is inherent to retinal cells. Therefore, we were also interested in the following question: If the irregularities in the spike trains are not related to noise, what kind of information do these irregularities carry?

II. METHODS

A. Single Circuit

Fig. 1(a) presents an electrical equivalent model of a two-channel neuronal membrane. In real neurons, potassium (K) and sodium (Na) conductances are time and voltage dependent. Hence, we can express membrane potential as follows:

$$C \frac{dV}{dt} = -G_K(V - V_K) - G_{Na}V + I_o$$

where C is membrane capacitance, V is membrane potential, G_K is potassium conductance, V_K is the equilibrium potential for potassium, G_{Na} is sodium conductance, and I_o is external current.

The membrane model from Fig. 1(a) can be generalized and simplified to the FitzHugh–Nagumo equations [(1a) and (1b)].

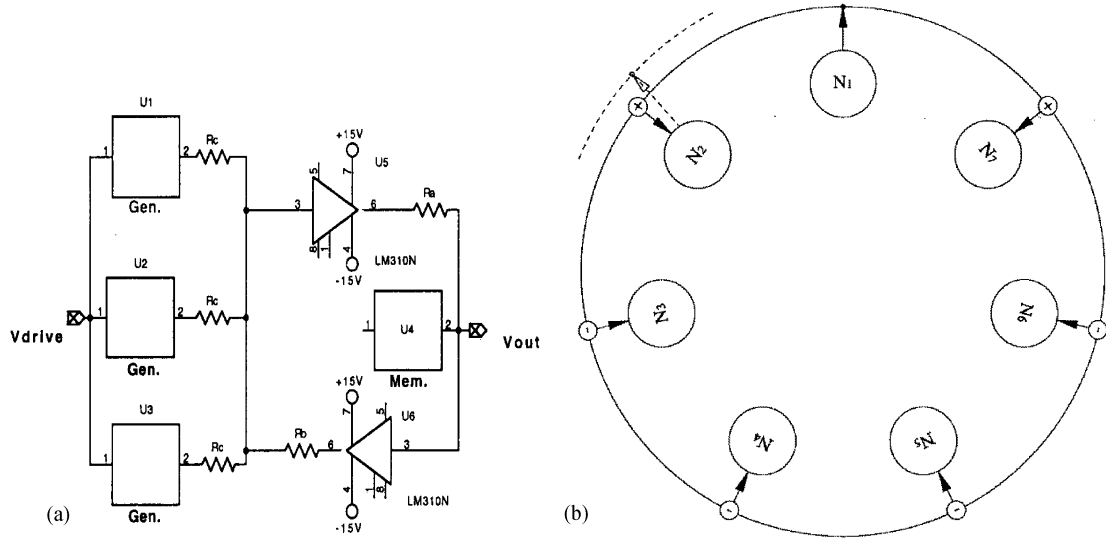


Fig. 2. (a) Schematic of the ganglion cell hardware model (G -neuron), which combines four oscillators ($U1-U4$) of the type shown in Fig. 1(b). In the retina, oscillators $U1-U3$ do not generate spikes and they are presynaptic to ganglion cells (oscillator $U4$). (b) Seven-cell neural network in which each neuron excites its two nearest neighbors (+), and inhibits all other neurons (-). These cells represent spiking ganglion cells in the retina. Their connections are related to gap junctions between ganglion cells or between ganglion and amacrine cells, as discussed in Section II-C.

We utilize an analog circuit designed by Keener [54] as a basic subunit for our hardware G -neurons. This analog circuit models Bonhöffer-van der Pol or FitzHugh-Nagumo equations

$$\epsilon \frac{dV}{dt} = I_o - I - G(V) \quad (1a)$$

$$\frac{dI}{dt} = \beta V - I - V_o \quad (1b)$$

where $\epsilon \in [0.01, 0.5]$ is a positive constant determining the nonlinearity (lower values of ϵ corresponding to higher nonlinearity), V is the voltage that models cell membrane potential, and I is the membrane current. $G(V)$ is a piecewise linear function which approximates a cubic polynomial [Fig. 1(b)]

$$-G(V) = \begin{cases} 1 - V, & \text{if } V \geq \frac{1}{(1+s)} \\ sV, & \text{if } -\frac{1}{(1+s)} < V < \frac{1}{(1+s)} \\ -1 - V, & \text{if } V \leq -\frac{1}{(1+s)} \end{cases}$$

where $s = 0.71$, $I_o = -0.5$, $V_o = -0.2$, and $\beta = 1.6$ are constants, with V_o determining resting equilibrium potential [fixed point or limit cycle; shown as a dot in Fig. 1(b)], and I_o is an externally modulated input.

Fig. 1(b) represents limit cycle oscillations described by (1a) and (1b). There are two nullclines which determine the trajectory of the oscillations. If we set (1a) to zero, we will get the first nullcline $dV/dt = 0$, with a characteristic S-shaped nonlinearity. By setting (1b) to zero, we will get the second nullcline where $dI/dt = 0$, which is a line with the slope β . The point where the nullclines cross determines the equilibrium state of the system. In Fig. 1(b), the equilibrium point is stable (this is known as an *excitable state*). Changes in the external current I_o shift the S-shaped nullcline up and down, while changes in the external voltage V_o shift the nullcline with a slope β in a

left-right direction. If we add positive voltage to the input, the nullcline with slope β moves to the right, and when it reaches knee of the S-shaped nullcline, the equilibrium point becomes unstable [shown as a dot in Fig. 1(b)]. This will start a limit cycle oscillation. A similar effect can be obtained by adding an input current and pushing the S-shaped nullcline upward.

By appropriate parameter choice, this circuit can model retinal circuits or cells showing rhythmic activity that mimic ganglion cell membrane properties [41].

B. G -Neuron

1) *Physiological Correlates*: An electronic analog of a single, isolated ganglion cell (G -neuron) consists of four resistively coupled circuits [Fig. 2(a)]. These oscillators have different eigenfrequencies, with ratios (1:8:24:40). Three of them have small nonlinearities ($\epsilon = 0.2$) whereas the fourth, fastest oscillator is characterized by a large nonlinearity ($\epsilon = 0.01$).

2) *Membrane Oscillator*: The fastest oscillator with a large nonlinearity generates signals similar to ganglion cell membrane potentials. The ganglion cell's membrane properties have been simplified. In the model, membrane properties related to integration of inhibitory postsynaptic potentials (IPSPs) and excitatory postsynaptic potentials (EPSPs) from the dendrites and cell body are reduced to a single point. Membrane permeability is simplified to the two-ion channels characterized by properties of the sodium and potassium currents [Fig. 1(a)]. The slow potassium current i_K is approximated by a linear function. The sodium current i_{Na} is fast and it has N-shape nonlinear characteristics as a function of the membrane potential [Fig. 1(b)]. Depending on the value of the potassium potential, the circuit oscillates spontaneously or is excitable [Fig. 1(b)].

3) *Intraretinal Oscillators*: The properties of three oscillators with small nonlinearities are related to the intraretinal oscillations. As described in the Introduction, the slowest oscillators are probably related to the horizontal cells network and in

the model they are represented by an oscillator with eigenfrequency = 1. The faster generator with eigenfrequency = 8 may be related to the amacrine cells' properties. The faster generator (eigenfrequency = 24) may be related to bipolar cells. In this paper, we selected frequencies of 6, 48, and 144 Hz for these three oscillators, matching the ranges of frequencies observed in the corresponding cell types, as summarized in the Introduction.

4) *Driving Signal*: The three generator potential oscillators [on the left side of Fig. 2(a)] are driven simultaneously by the input voltage signal V_{drive} . The driving signal simulates the signal from the photoreceptors, which in our model is proportional to light intensity. Photoreceptors have synapses with the bipolar and horizontal cells. Only bipolar and amacrine cells have direct synapses with the ganglion cells. Therefore, our model simplifies retinal connections. The outputs of the three generators are resistively coupled to a common point, which corresponds to the G -neuron's overall generator potential.

5) *Antidromic Propagation of Action Potentials*: The generator potential is a sum of the EPSPs and IPSPs. The action potentials are generated in the axon hillock, the initial narrow part of the axon with the highest density of Na^+ channels and lowest threshold [55]. Spikes generated in the axon hillock spread in two directions: along the axon (orthodromic direction), and into the soma and dendritic tree (antidromic direction) [56]. In the G -neuron, as in the retinal ganglion cells, the oscillator that simulates generation of the action potentials is strongly driven by the generator potential, and in turn has a relatively smaller influence on the generator potential itself.

6) *Implementation*: One advantage of using hardware is that it is possible to scale the speed of the circuit to accelerate sampling, while preserving the overall network characteristics. In order to shorten simulation time, the frequencies of all oscillators were scaled up ten times higher than in the retina to the following frequencies: 60 Hz : 480 Hz : 1.44 kHz : 2.4 kHz. As described previously, the three oscillator corresponding to intraretinal processes are connected in parallel and driven from a single source V_{drive} [Fig. 2(a)]. The output of the oscillators drives the membrane oscillator. Replicating the antidromic spread of action potentials, the membrane oscillator gives feedback to the three slower oscillators. The antidromic coupling is attenuated relative to the orthodromic coupling by means of buffer amplifiers $U5$ and $U6$ and the corresponding resistors R_a and R_b [with $R_a > R_b$ in Fig. 2(a)].

Each oscillator can be described by (1a) and (1b) with the nonlinearity coefficient ϵ and different period of oscillation as described previously. Coupling will modify equations in the following ways.

Oscillator $U1$:

$$\epsilon_1 \frac{dV_1}{dt} = I_{o1} + \frac{V_2}{R_c} + \frac{V_3}{R_c} + \frac{V_4}{R_b} - I_1 - G(V_1) \quad (2a)$$

$$\frac{dI_1}{dt} = \beta_1 V_1 - I_1 - V_{o1}. \quad (2b)$$

Oscillator $U2$:

$$\epsilon_2 \frac{dV_2}{dt} = I_{o2} + \frac{V_1}{R_c} + \frac{V_3}{R_c} + \frac{V_4}{R_b} - I_2 - G(V_2) \quad (2c)$$

$$\frac{dI_2}{dt} = \beta_2 V_2 - I_2 - V_{o2}. \quad (2d)$$

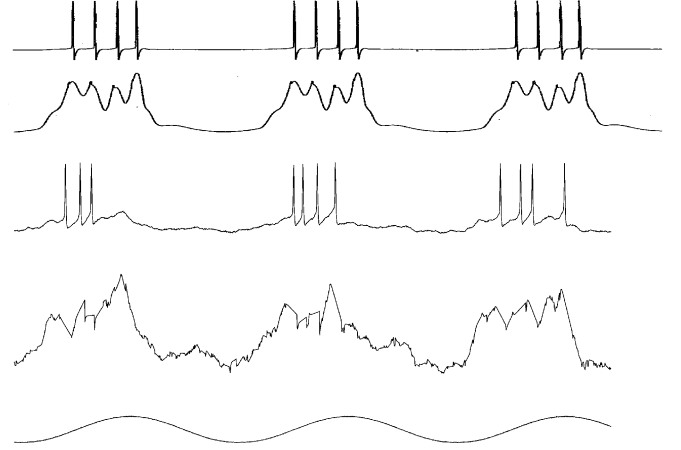


Fig. 3. Comparison between intracellularly measured ganglion cell activity in the cat (middle two traces) and the response of the G -neuron (top two traces) to a sinusoidal input (bottom trace). As described in [13], the cat was under pentobarbital anaesthesia, artificially ventilated. A glass pipette microelectrode was used to record intracellular ganglion cell activity in the optically intact *in situ* eye, while the eye was stimulated with spots of light sinusoidally modulated in intensity. The generator potential was extracted using a wavelet method [12] (as a sum of input signals; fourth trace from the top) from the intracellular membrane potential (third trace from the top) [13]. All signal amplitudes were normalized. The frequency of the sinusoidal input is 16 Hz for the cat and 160 Hz (scaled ten times) for the model.

Oscillator $U3$:

$$\epsilon_3 \frac{dV_3}{dt} = I_{o3} + \frac{V_2}{R_c} + \frac{V_1}{R_c} + \frac{V_4}{R_b} - I_3 - G(V_3) \quad (2e)$$

$$\frac{dI_3}{dt} = \beta_3 V_3 - I_3 - V_{o3}. \quad (2f)$$

Membrane oscillator $U4$:

$$\epsilon_4 \frac{dV_4}{dt} = I_{o4} + \frac{V_1}{R_a} + \frac{V_2}{R_a} + \frac{V_3}{R_a} - I_4 - G(V_4) \quad (2g)$$

$$\frac{dI_4}{dt} = \beta_4 V_4 - I_4 - V_{o4} \quad (2h)$$

where the coefficient β and the nonlinear function G are the same as in (1a) and (1b); $\epsilon_1 = \epsilon_1 = \epsilon_1 = 0.2$, $\epsilon_4 = 0.01$, R_c is related to the coupling coefficient between the three presynaptic oscillators, R_a is related to the coupling coefficient from the presynaptic oscillators to the membrane of the ganglion cell oscillator, and R_b is related to the feedback from the action potential generated in the axon hillock to the membrane generator potential (see Section II-B5).

7) *Model Parameters*: The parameters of the hardware circuit were tuned to simulate light responses of retinal ganglion cells. For example, Fig. 3 shows the intracellular recordings of a single ganglion cell in the retina *in vivo*, along with the response of a single, isolated G -neuron. In this case, the input consists of a sinusoidally modulated light spot (Fig. 3, bottom trace). In Fig. 3, the second trace from the top represents voltage amplitude changes in the model; and the fourth trace from the top shows the generator potential recorded from the retina. Slow responses locked to the stimulus and fast oscillations of the generator potential in the retina are similar to voltage changes in the hardware circuit (fourth and second trace from the top). Spike trains in the model (top trace) and in the retina (third trace

from the top) show similar one-per-stimulus period bursting, although in the retina the bursts are less regular. As we have shown in [57], one source of the burst modulation that is not captured in the hardware model is related to slower membrane ion channels. Another source may be related to the interactions between ganglion cells [58].

C. *G*-Network: Network of Coupled *G*-Neurons

1) *Physiological Evidence*: To simulate a simplified center-surround circuit, our hardware model consists of a ring of seven resistively coupled *G*-neurons [Fig. 2(b)]. Each *G*-neuron is coupled to its two nearest neighbors with strong excitation, and to all other neurons with inhibition.

There is no evidence that retinal ganglion cells make chemical synapses in mammalian retinas. However, there is strong evidence from the Limulus [59] to primate retina about the lateral inhibition network formed by eccentric (ganglion) cells. In primates, the lateral inhibition network is built by gap junctions between parasol and amacrine cells [60], [61]. According to the model of Kenyon and Marshak [60], the small amacrine cells disinhibit parasol cells, whereas the axons of the large amacrine cells inhibit parasol cells over a large area of the retina [60]. As one consequence of these coupling, synchronized firing between ganglion cells in primate retina were modeled [108] and experimentally confirmed [62].

Similar effects were recorded in the cat, rabbit, and salamander retinal ganglion cells. Multielectrode recordings from cat [63]–[65], rabbit [66], and salamander [67], [68] retina have shown tightly correlated activity of adjacent ganglion cells and much weaker activity for distant pairs [64]. The strongest correlations were between neighboring *Y*-cells (cells with large overlapping receptive fields); the weakest were between *X*-cells (cells with small receptive fields) [64]. It is likely that reciprocal correlations occur through electrical synapses [61], [65], [67], [69]–[72]. The correlations between maintained firing are probably caused by shared active inputs, which are likely to be related to spiking amacrine cells [65].

2) *Implementation*: As shown in Fig. 2(b), *G*-neuron N1 gives excitatory (+) connections to two *G*-neurons N2 and N7. These excitatory connections are three times stronger than the inhibition (−) to all other neurons N3–N6. Both excitatory and inhibitory connections are realized through subthreshold (without spikes) coupling of the potential. The output of the three oscillators in N1 (analog of the generator potential in the ganglion cells) is connected to two amplifiers, one of which is inverted to simulate inhibitory connections. The outputs of both amplifiers are scaled appropriately by resistors and connected to the inputs of other *G*-neurons. Similar connections are made for all other neurons as indicated by the dotted line for the N2 cell in Fig. 2(b).

D. Data Analysis

In order to validate our model we have compared signals from the model to experimental recordings found in the literature and obtained in our laboratory. We have analyzed: 1) spontaneous (maintained) activity when the input signal was direct current (dc) with 0 (dark) or higher (constant illumination) amplitude,

and 2) evoked activity when the input signal has a dominating alternating current (ac) component (such as, for example, sinusoidal modulation of the retinal illumination).

1) *Statistical Analysis*:

a) *Analysis of the spike interval variability*: Spontaneous activity in retinal ganglion cells has often been tested by statistical methods [73]–[75]. Several labs [73], [74], [76] were interested in how the next spike interval is determined by the preceding interval. They have found that the serial statistical dependency of interspike intervals is weak and variable.

Frishman and Levine [77] have divided the relationship between spike intervals into short- and long-term dependencies. Both were found to be weak, but the short-term dependency was independent on the level of illumination, whereas the long-term dependency increased at higher levels of illuminations. The authors proposed a model with two sources of noise: distal and proximal (for details, see Section IV). Levine [75] noticed that the interval between spikes in the maintained discharges were better approximated by a log-normal distribution than other distributions. For example, the gamma distribution applied by Kuffler *et al.* [78] does not extend to frequently observed very long interspike intervals.

Based on these and other findings, Levine and Zimmermann [79] proposed a model for the variability of interspike intervals during periods of maintained discharge. They characterized the variability by the coefficient of variation (CV) = s/m , the ratio of the standard deviation of intervals between successive impulses to the mean interval between impulses. This model [79], when data are plotted in log–log coordinates, explains that maintained discharge can derive its variability from linearly added noise in the steady-state conditions, and from nonlinear interactions in response to abrupt changes in illumination. Levine *et al.*'s analysis of the maintained ganglion cell activity compared different statistical tests on a large amount of experimental data, and it is, therefore, a good basis for our model verification.

b) *Coefficient of the bursting regularities*: A spike burst was defined as a group of spikes separated by the longest silent periods (spike interval) in each stimulus cycle [57]. Burst duration was defined as a sum of all interspike intervals within a single burst. The coefficient of the bursting regularity was defined as the inverse of the burst irregularity [57]. Burst irregularity (b_{irr}) is the standard deviation of the burst duration (SD_{tb}), divided by the ratio of the average burst duration ($\text{mean}(tb)$) to the duration of one stimulus period T ; $b_{irr} = SD_{tb}/(\text{mean}(tb)/T)$. Burst regularity is equivalent to an inverse of the standard deviation of the normalized burst duration.

2) *Dynamical Systems Analysis*: In addition to the statistical measures popular in neurophysiology as described previously, we have characterized the responses of the model using dynamical systems analysis.

a) *Parameter space scan*: Takahashi *et al.* [80] characterized the parameter space for the membrane of the squid axon. The axon was periodically stimulated and its responses were characterized by changing the stimulating current intensity and the current pulse intervals [80]. We have performed a similar search for a single Keener circuit and for a network of *G*-neurons.

The periodicity of the signal in the Keener circuit (Fig. 4) or the periodicity of the pulse train in the G -neuron (Figs. 9 and 10) are plotted as a function of the frequency and amplitude of the driving source [81], [82]. The data were sampled at the drive frequency. Period 1 repeated every sample; period 2 repeated every other sample, etc. The root mean square (rms) error of the samples had to be within a small error range to count as periodic. In other words, if response of the circuit repeats for every period of the input signal, then the output is synchronized to the input with period 1. If the circuit response repeats every second period of the input signal, then the output is synchronized to input with period 2, etc. If circuit responses are changing with each period of the input signal then the circuit shows quasi-periodic or chaotic oscillations. This method of analysis is very popular in the dynamical systems area with many experimental applications, e.g., [81], [82]).

However, for the spike (pulse) train responses (Figs. 9 and 10) we modified the aforementioned method using the spike coincidence method. At first, we plotted the number of spikes as a function of the stimulus interval length. If the number of spikes in each stimulus period was the same, then we had period 1 response; if number of spikes was the same every two periods of stimulation, then we had synchronized response with period 2, etc. (see Figs. 9 and 10, for examples). This is similar to the previously described method, but instead of using the analog value of the output signal we use the number of spikes. However, this method does not tell us how many spikes are in each period of the stimulus, and whether the spikes or burst of spikes are regular within each period of the input signal (see also burst regularity paragraph (Fig. 3) and experimental data in [9] and [26]). Therefore, we have divided each period of the input signal into subperiods and checked, for a large number of periods of the stimulus, whether each spike falls into the same subperiod (coincidence method). If this was the case, then the circuit was said to respond with period 1, but with a higher number of spikes (marked with darker colors in Figs. 9 and 10) in each period of the input signal.

b) Close return histogram: Pulses simulating ganglion cell spikes were generated by G -neurons and encoded into single-bit 0–1 trains. For the spontaneous, nondriven activity, we have applied the *close return histogram* technique. This technique from dynamical systems theory, originally proposed by Lathrop and Kostelich [83], was applied to the interpulse intervals I_k , $k = 1, 2, \dots, N$. A window size ω was chosen and a histogram was created by counting, for each delay n , the number of times the condition $|I_k - I_{k+n}| < \omega$ was true.

For the first delay, the number of spikes within this window was calculated for all k . In the next step, the delay was increased, and again number of spikes with this delay (period) was calculated for all k . This procedure was repeated until period 100. The maxima in the close return histogram are related to unstable periodic orbits in the time series [83]. The unstable periodic orbits are periodic orbits embedded in the chaotic attractor. This measure is based on the fact that unstable periodic orbits are related to saddle orbits, which are characterized by attracting and repelling directions. Trajectories approach the saddle orbits along the attracting direction and remain nearby before they are pushed away. We assume that when a trajectory is near the

saddle orbit, the resulting spikes (pulses) have similar intervals, with a difference within the window size ω which depends on how closely trajectory approaches a saddle orbit [83].

III. RESULTS

A. Single Keener Circuit Responses

In order to characterize the behavior of the Keener circuit, a single circuit [Fig. 1(a)] was driven with a sine wave of variable amplitude and frequency. The result of a parameter space scan is shown in Fig. 4. The response of the circuit was sampled on a 100×100 grid of amplitude and frequency, and color-coded according to the period of the circuit response relative to the period of the driving sine wave. The resulting plot exhibits a number of color “tongues,” i.e., areas of the response space that share a common periodicity. The periods of several prominent tongues have been shown; the most visible are period 1 on the left (maroon) and period 2 on the right (yellow). For period 2 the driving potential completes two cycles in the time it takes the circuit to complete one. The white zone represents quasi-periodic responses; that is, the circuit and the sine wave do not phase-lock and remain individually periodic and uncorrelated. The ordering of the tongues and their periods is typical of a two-frequency quasi-periodic system (see, for example, [20] and references therein). The random scatter of colored points throughout the white zone and in the tongues is due to inefficiencies in the on-line computer algorithm used to perform the scan. No attempt was made to thermally stabilize the circuit, resulting in the slight “snakeiness” and occasional discontinuities that are especially apparent when the tongues are thin.

B. Spontaneous Oscillations in the G -Neuron Network

In order to simulate ganglion cell spontaneous activity, the limit cycle was chosen as a resting state of each generator potential oscillator. Coupled G -neurons generated pulse trains that are different for each of the seven coupled neurons [Fig. 5(a)]. These differences are related to small variations in their setups, their components, and inhibitory connections between them [Fig. 2(b)]. G -neuron activity in Fig. 5(a) looks similar to the maintained ganglion cell multiunit activity recorded in darkness from the salamander retina [84]. Spontaneous activity in the salamander retina is slower than in the cat, but it shows limited time and space synchronization between different cells as in Fig. 5(a).

1) Statistical Analysis: In Section II, we reviewed the statistical methods used to analyze maintained activity in the retinal ganglion cells. Levine [75] found that a log-normal distribution provides the best fit to the ganglion cell maintained discharges. We did similar calculations for pulses generated by G -neurons when a dc (constant) input signal was set between 0–0.4 V. As found in ganglion cells [75], [85], [86], the interval distribution histogram of pulses generated by G -neurons fit the log normal distribution well. In Fig. 6, we have plotted the coefficient of variation as a function of the mean spike rate in logarithmic coordinates. Experimental data for different ganglion cells were approximated by a power function: $CV = ar^{0.5}$ where r is the mean spike rate [75]. In our plot of $\log(CV) = f(\log(r))$, we have found a similar slope to that described for the cat ganglion cells. Our 95% confidence interval for the slope was $(-0.6561,$

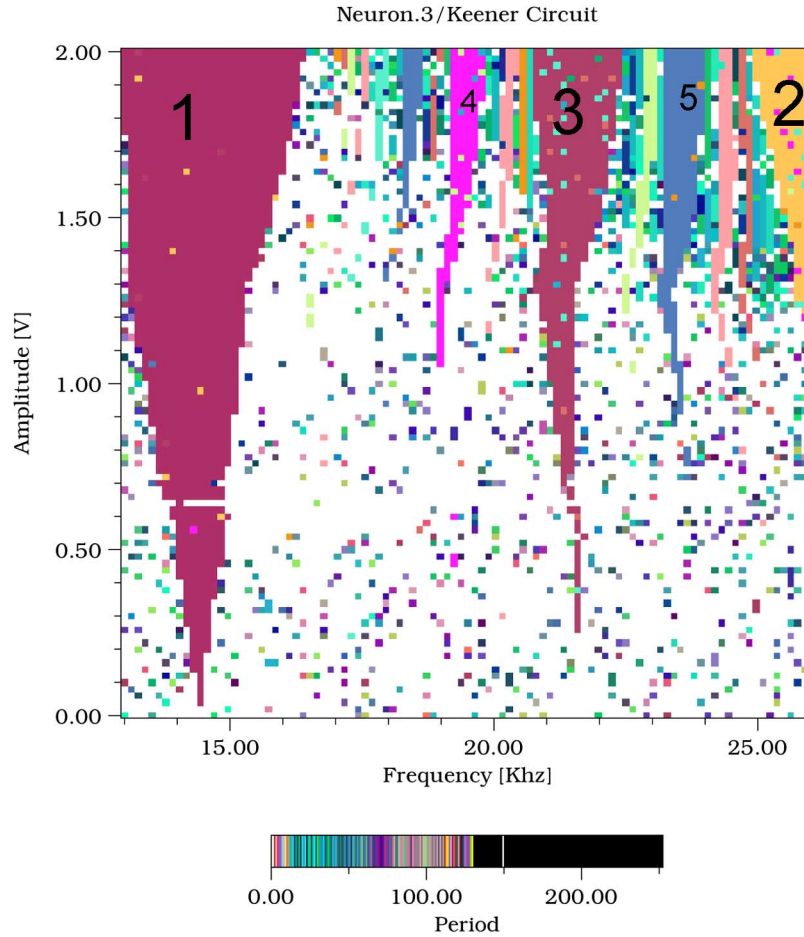


Fig. 4. Parameter scan of the response of the Keener circuit driven with a sine wave of variable frequency and amplitude. The response is sampled on a 100×100 grid of amplitude and frequency. Color coding is used to highlight periodicity relative to that of the driving sine wave. The biggest tongue on the left (maroon) represents period 1. On the right of the figure part of the tongue of period 2 is visible (yellow). Other periods in the figure include: period 3 in light maroon, period 4 in purple, and period 5 in dark blue. Other periods show increasingly small tongues.

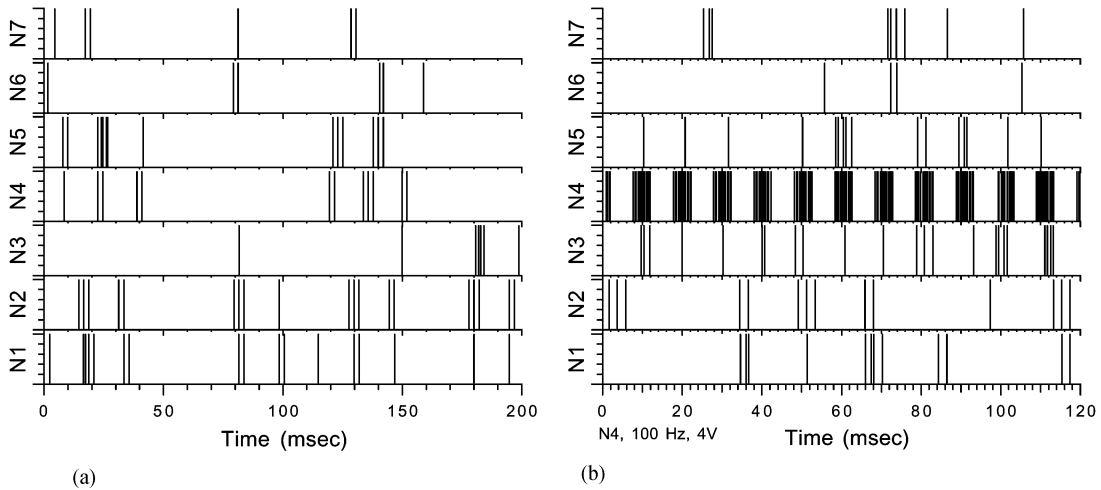


Fig. 5. (a) Spontaneous activity of seven *G*-neurons represented by irregular pulses in time. (b) Activity of the same *G*-neurons when one of them (N4) is forced with sinusoidal input.

-0.5029), while the slope calculated for 13 ganglion cells in the cat was -0.51 [38] and -0.55 or -0.59 for different types of anaesthesia [39].

2) *Dynamical Systems Analysis*: In Section II, we explained that the close return histogram [83] can classify how periodic or

aperiodic the pulse train is. As discussed previously, the pulse trains generated by our model have similar statistical properties to the maintained activity of retinal ganglion cells. We were interested in finding out what periodicity can be expected in the pulse train generated by the network when there is no input

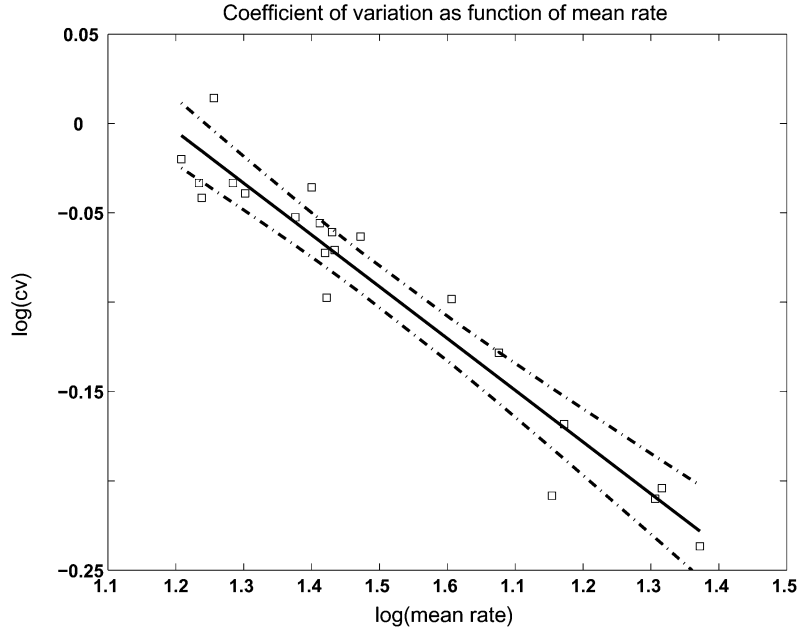


Fig. 6. Statistical analysis of spontaneous activity in G -neurons. Log-log plot of the CV as a function of the mean rate (r) between impulses (circles). The best fit was $CV = ar^{-0.579}$, shown here as a continuous line. The dashed lines show the 95% confidence interval.

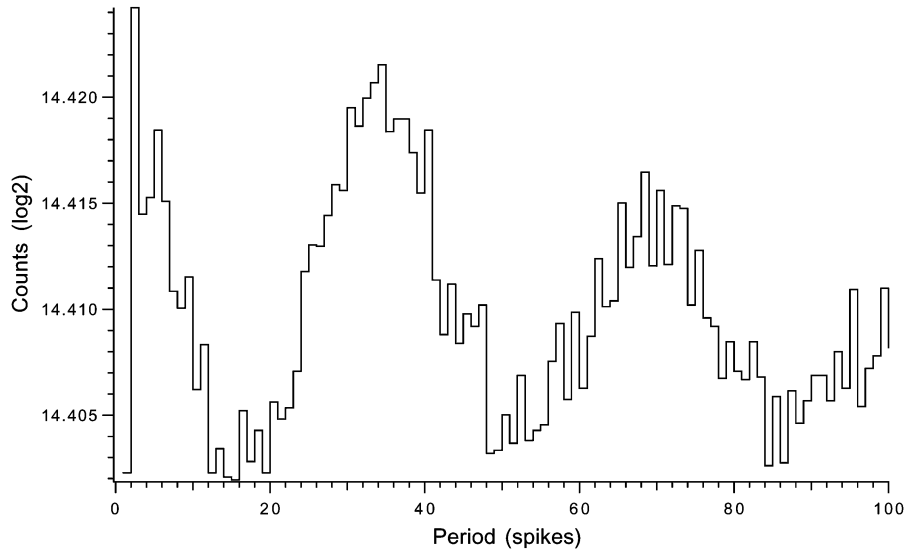


Fig. 7. Close return histogram for spontaneous activity of G -neuron N4 (25 000 spikes). The x -axis shows recurrent time n as the delay between spikes (see Section II-D2b), while the y -axis shows the number of points (times) when the difference between spike intervals is small (within the ω window size—Section II).

signal driving the circuit. As described in Section II, we calculated the number of spikes within periods growing from 1 to 100. We have found that the interval distribution histogram in the pulse train generated by our model exhibits periodicity (period 1) for a delay of $n = 32$, which is equivalent to 57.5 ms (Fig. 7). This is the shortest period orbit, referred to as the *period 1 saddle* [83]. Fig. 7 also shows an orbit with period 2 (local maximum at $n = 64$). This reflects the existence of unstable periodic orbits, suggesting quasi-periodic or chaotic underlying dynamics in the coupled generators.

C. G -Network Responses to Sinusoidal Driving of G -Neurons

1) *Spike Train Changes*: A sinusoidal input applied to one of the G -neurons (N4) strongly increased regularities in the ac-

tivity of most G -neurons [Fig. 5(b)]. The nearest neighbors (N3 and N5) of the driven G -neuron showed stimulus-locked activity with the input. Other G -neurons showed a more complicated relation to the stimulus: G -neurons N2 and N6 generated spikes most frequently in counterphase with G -neurons N3 and N5. N1 and N7 were even less correlated to the input, but were also largely in counterphase. Driving three G -neurons simultaneously (N3-N5) phase-locked them strongly and inhibited N2 and N6 units, which were mostly active in phase with the input. N1 and N7 were lightly excited and active in counterphase to the input. We have driven with a sinusoidal signal a single G -neuron (N1), or two G -neurons (N1 and N2), or more, up to all seven G -neurons, and calculated regularities of the bursting in the N1 G -neuron. We have calculated pulse burst regularities in the

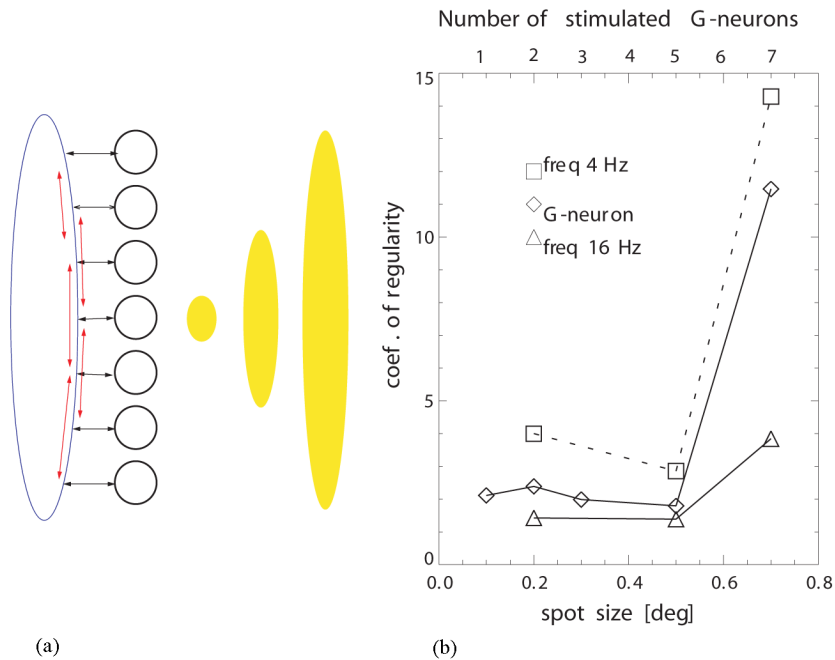


Fig. 8. (a) Schematic picture represents G -network stimulation with different sizes of light spots. (b) Coefficient of the burst regularity (inverse of normalized standard deviation of the burst duration; see Section II) as a function of the spot size. In experiments on a cat, the spot size is represented in degrees, while in the model the spot size was related to stimulation of 1, 2, 3, 5, or all 7 G -neurons. A spike burst was defined as a group of spikes separated by the longest silent period in each stimulus cycle. Burst duration was defined as a sum of the interspike intervals in the burst. Comparison of the data measured in the cat retina *in vivo* as described in Fig. 3 [13], [57] at temporal frequencies 4 and 16 Hz and measurements in the model (middle trace for the G -neuron).

model and compared them with the spike burst regularities in the cat ganglion cell obtained by changing the light spot size from 0.2° to 0.7° as schematically shown in Fig. 8(a). Fig. 8(b) shows measurements from a retinal ganglion cell and from the model. Increasing of the stimulus size (in our model, corresponding to an increase in the number of stimulated G -neurons) caused at first a decrease, and subsequently a very strong increase in the response regularity in the ganglion cells and in the model.

2) *Complex Structure of the Network Activity*: We have analyzed G -network responses to sinusoidal inputs using the coincidence algorithm. We have sinusoidally stimulated one G -neuron and counted the number of spikes in intervals ranging from very narrow (exact spike coincidence) to the size of stimulating period. We have coded the number of spikes in each interval in intensity (darker = more spike) and plotted the interval size as a function of the signal frequency input (Figs. 9 and 10). In Fig. 9, the same G -neuron was driven and analyzed [N1 neuron in Fig. 2(b)]. Period 1 oscillations synchronized with the stimulus were dominating in Fig. 9. A driving signal with frequency between 120–160 Hz (12–16 Hz in the retina) and small amplitudes evoked period 2 oscillations (drivers complete two cycles when pulse train shows only one cycle). The period 3 oscillations dominated only in a very small range of frequency–amplitude parameters.

However, neighboring neurons show a completely different behavior. For example, in Fig. 10, one G -neuron (N1) was driven and the neighboring neuron [N2 in Fig. 2(b)] was analyzed. In the neighboring G -neuron, as shown in Fig. 10, many different oscillations interleaved in a manner which resembles “Arnold tongues” observed in a single Keener circuit (Fig. 4). However, a more careful analysis showed that in this map, cones

with various periods were strongly deformed Arnold tongues. Period 1 oscillations had one dominating peak around 60 Hz and another one around 30 Hz (the slowest oscillator in the network is 60 Hz; it is related to the 6-Hz oscillator in the retina). Two period-3 cones were: the first one around 90–100 Hz and the second one around 180 and 210 Hz (9–10 Hz, and 18–21 Hz in the retina). Similarly, period-2 and period-5 cones showed double peaks.

Therefore, the cones in the frequency–amplitude parameter space for the network (Fig. 10) were relatively wider and had different shapes than the cones observed in the isolated Keener circuit (Fig. 4). Also, scaling of the cone amplitude for the network is different than for the Keener circuit. In the network (Fig. 10), sensitivity to all periodic oscillations is almost similar, whereas in the Keener circuit, the cone size decreased when the period number increases. This could be the reason why multi-period oscillations were experimentally observed (e.g., [12]).

IV. DISCUSSION

A. Single Neuron Properties

Whether modeling brain function or building brain implants, a fundamental question is: How complicated should the properties of a single neuron be? In this section, we will describe and discuss several simple models of neurons based on cell membrane properties.

The simplest model of the membrane properties of a neuron is based on the original proposal of McCulloch–Pitts, which sums signals between threshold and saturation. The output of this model is a continuous function related to the spike rate of the real neuron.

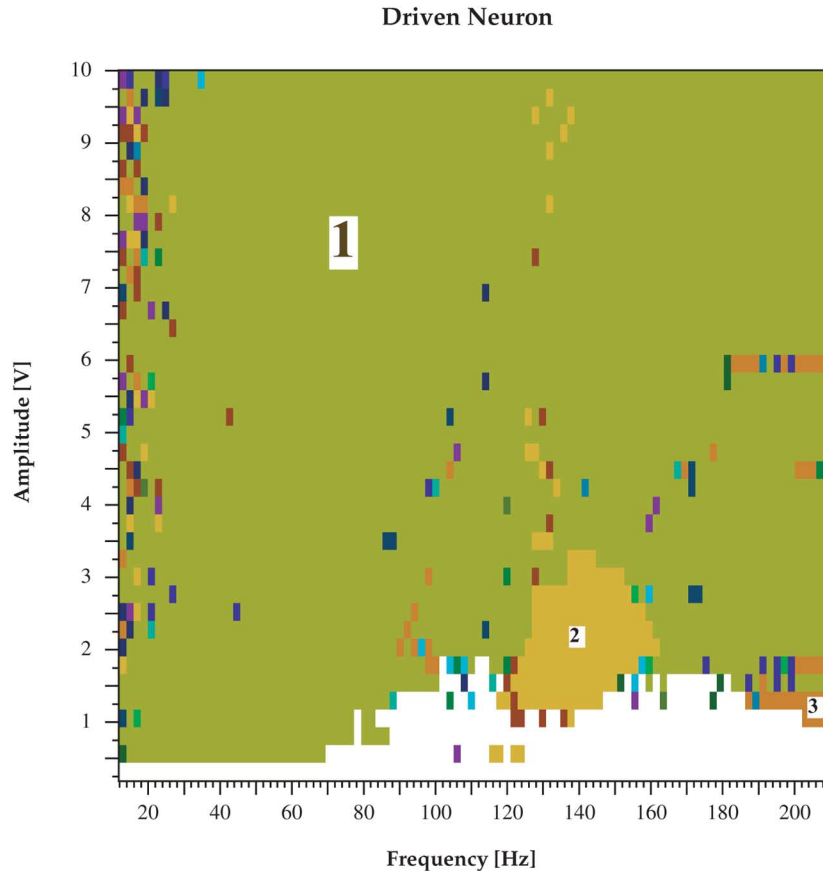


Fig. 9. Spike coincidence response of the G -neuron network driven with a sine wave of variable amplitude and frequency. Driven neuron responses are shown. Response is sampled on a 40×100 grid of amplitude and frequency. Color coding is used to highlight the number of spikes in each interval relative to the driving sinusoid. If the number of spikes is the same in each period of the driving signal, then network response is synchronized with input with period 1. If the number of spikes repeat with every second period of the input signal, then the circuit oscillation has period 2, etc. The first three periods are labeled; higher order periods have darker colors.

A modification of this model, known as the *integrate-and-fire* neuron, generates a short pulse (spike) when the sum of the input signals reaches a threshold. A possible output of this model is a train of simulated spikes. However, both the McCulloch–Pitts and integrate-and-fire models do not capture dynamics related to action potential generation.

A modification of the integrate-and-fire model, the *leaky integrate-and-fire* neuron, introduces a time constant $\tau = RC$ as a product of the capacitance C and leak resistance R of the cell's membrane. After spike generation and reset of the membrane potential (V_m), the prevailing input leads to a decay of the potential V_m with the leak time constant τ . This process simulates a refractory period during which the probability of spike generation is reduced.

The leaky integrate-and-fire model has been successfully used to simulate the spike generation mechanism of retinal ganglion cells [50], [87]. In a previous paper, we have improved Lankheet's model [87] by replacing the leaky integrator with a cell membrane multi-ion channel model based on patch-clamp experiments [57].

In this paper, membrane properties were limited to two-ion channels using sodium and potassium channels, with properties defined by the nonlinear differential equations proposed by FitzHugh [88], and implemented by Keener [53]. An equivalent model was recently proposed in [105]. In the following, we will

explain why introducing membrane properties related to the ion channels, as analyzed in the stimulus related parameter space, is crucial for our model.

As we have shown in Fig. 4, our model shows a characteristic property in the frequency–amplitude parameter space: Arnold tongues. In order to reveal this property, we scanned the parameter space by changing input signal frequency and amplitude (10 000 different values) and analyzed circuit responses to each signal. As explained previously, the circuit response is said to have period 1 if the response is synchronized with each period of the input signal, period 2 if the response is synchronized with every other period of stimulation, and so on. If the response does not repeat, the output signal is not synchronized with the input (white area in Fig. 4). Notice that when the amplitude of the input signal is larger, then the circuit responses have wider range of synchronization. This is evident in Fig. 4 by observing that the areas of constant periodicity have a conical shape. As one can notice in Fig. 4, noise causes deformation of the cones. These deformations are more significant for lower amplitudes and higher frequencies in the input signal. In the retina, adaptation processes guarantee sufficiently large amplitude. Therefore, noise will have more significant influence on oscillations of higher order. One option to decrease the negative effect of the noise is to create (possibly by learning in the higher brain areas) appropriate oscillating circuits tuned to the significant frequencies.

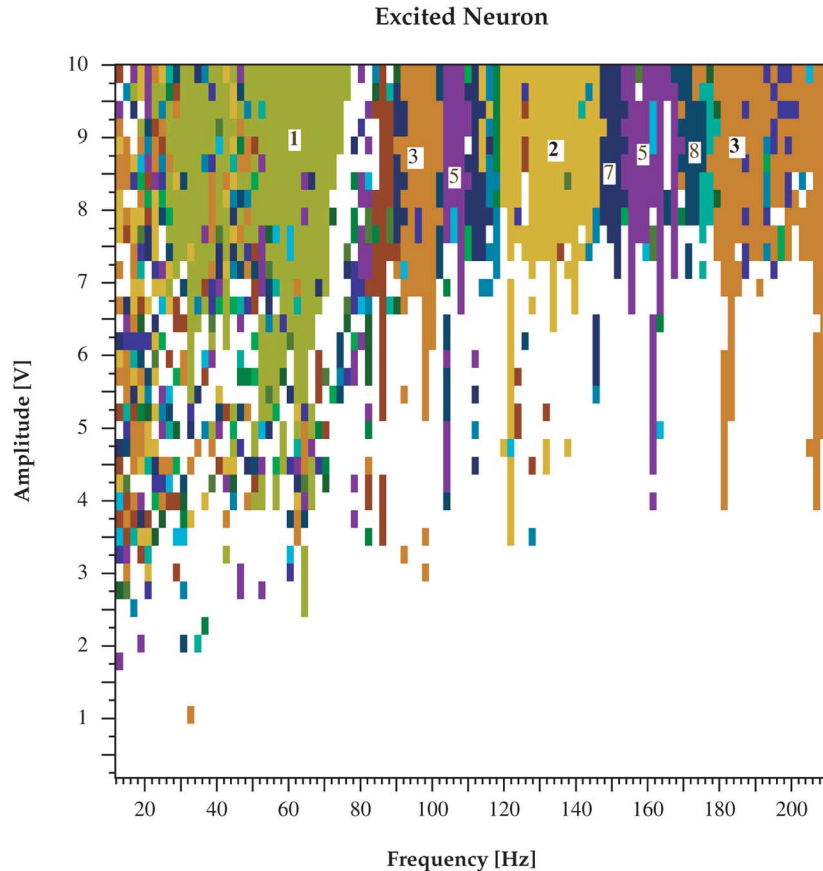


Fig. 10. Spike coincidence response of the G -neuron network driven with a sine wave of variable amplitude and frequency. Responses of near neighbors of the driven neuron are shown. Response is sampled on a 40×100 grid of amplitude and frequency. Color coding is used to highlight the number of spikes in each interval relative to the driving sinusoid. The first several periods are labeled; higher order periods have darker colors.

The order evident in the Arnold tongues shows characteristic period adding, whereby adding the periods of two larger cones gives the period of the cone between them. For instance, the largest cone represents period 1 ($1p$) oscillations (Fig. 4), while the cone in the middle has period 3 ($3p$, third subharmonic) oscillations. The largest cone between them has period 4 ($1p + 3p$), the cone between $1p$ and $4p$ has period 5 ($5p$), etc. This is similar to physiological experimental findings from the squid axon [80], and to other experimental findings related to the one-dimensional (1-D) circle map model [89]. In the standard circle map, increasing nonlinearity k from zero to one increases regions where the solution is locked to the input frequency [89].

Nonlinearity in the circle map plays a similar role to the increase of the input amplitude in the FitzHugh–Nagumo equation [(1a) and (1b)]. In general, dissipative properties of the Hodgkin–Huxley membrane equations are responsible for the areas of periodic responses (frequency locking) represented by the Arnold tongues (Fig. 4).

As a consequence, synchronization is widespread in many brain structures. This means that for certain conditions, high-dimensional differential equations describing circuits of neurons have a low-dimensional solution (1-D for the limit cycle describing synchronization) [90]. Therefore, activity of the whole neuron population may divide into synchronized subpopulations. These subpopulations become adaptive units representing many parallel processes responsible for extraction of specific

attributes. Subpopulation synchrony will generate spikes by increases in the EPSP at the next stage neurons.

B. G -Neuron

We have built a hardware model of the ganglion cell (G -neuron) according to experimental data. Our G -neuron provides a reasonable replica of intracellular recordings from the cat retinal ganglion cells [13] and digital simulation of their responses to light flicker [57], [91].

Each G -neuron consists of four coupled nonlinear oscillators. Three oscillators are simulating intraretinal processes and the fourth one is related to the cell's membrane properties. The eigenfrequencies of all oscillators are similar to experimental data from the retina (see Introduction). As was described in Section II, neural circuits in the retina show behavior similar to the behavior of the hardware oscillators we have created (Fig. 3).

C. G -Network

In general, we have found many similarities between properties of the pulse train generated by our model and spike trains recorded from retinal ganglion cells. We have divided our analysis into two parts: 1) maintained network activity, and 2) driven network activity.

1) *Maintained Network Activity*: Statistical properties of the spontaneous activity in a cat ganglion cells [75], [79] have been compared to the maintained network activity of our G -neurons.

We have found that the spike intervals and coefficient of variation plotted as a function of mean spike rate have similar characteristics for the ganglion cells and for the G -neurons.

Frishman and Levine [77] have proposed that the variability (noise) in the maintained ganglion cell activity has two sources: a distal source and a proximal source. They did not exactly identify different noise sources, but distal noise seems not to be related to photoreceptor isomerization. Their restriction was that between the absorption of photons and the source of the noise there must be the low-pass filter. This filter can be within the photoreceptor or in the receptor-bipolar cell synapse. The noise generated in the distal retina and signals from photoreceptors after the high-pass filter interact with the second source of noise from the proximal retina.

This model could explain properties of the maintained activity at different levels of constant illumination. In our model, interactions between several intraretinal subsystems lead to similar results, but instead of noise modified by different filters [77], [92] we have introduced three different oscillators. From the experimental point of view, long and very stable continuous recordings are required to differentiate between noise, quasi-periodic oscillations, and chaos.

We have analyzed a 25 000-pulse train from our model by means of the close return histogram technique (Fig. 7) and found that maintained network activity consists of quasi-periodic or chaotic oscillations. Our results agree with the recent findings showing that very long periods of the maintained network activity in the cat retinal ganglion cells have fractal properties [93], [94].

Similarly to the retina, spontaneous activity of neurons in the primary visual cortex (V1) is variable and often assumed as noise or as playing no significant functional role [95]. However, there is evidence that it is not the case. Recently [96]–[98] and earlier [99], [100], researchers at Grinvald's Laboratory in Neurobiology Department, Weizmann Institute of Science, Rehovot, Israel, and elsewhere found that the pattern of spontaneous activity in the network surrounding a given neuron in V1, can predict the neuron's responses to different stimuli. By correlating spikes of the cell with the spontaneous activity of the neighboring network, one can find preferred network states that determine the preferred stimulus for the neuron. This provides further evidence for the importance of cell-level and network-level oscillations in the processing of information.

2) *Driven Network Activity:* Driven network activities registered in the G -neurons were compared to light flicker responses of the ganglion cells. We have found that in G -neuron networks, as in the retina, forcing even one G -neuron evoked responses synchronized with the stimulus [Fig. 5(b)], as is the case with stimulation of the receptive field of a single ganglion cell. Periodic stimulation increases the regularity in the spike train in comparison to spontaneous activity [Fig. 5(a)]. When the number of stimulated G -neurons or size of the stimulus in the retina was further increased, spike trains became even more regular [62].

We have quantified these observations by plotting the coefficient of spike burst regularity as a function of the spot size or number of stimulated G -neurons (Fig. 8). In our model and in the retina, we have observed similar changes in spike burst reg-

ularities: At first a decrease and later a strong increase of the regularity with the number of stimulated neurons. Others [12], [50], [51] have observed that when the whole retina was stimulated, repeating the same stimulus many times evoked identical responses each time. The spike trains recorded in ganglion cells in response to the diffuse flicker stimulus can be predicted with high precision by a model proposed by Keat *et al.* [52].

The first stage of the Keat *et al.* [52] model is a filter that consists of a sum of sinusoidal functions with adjusted amplitudes. The input of the filter is proportional to the amplitude of the light stimulus, and its output simulates the ganglion cell generator potential. The lowest frequency in their model of cat ganglion cells was about 4 Hz, which is in the same range as our slowest oscillator (6 Hz).

Our three intraretinal oscillators with small nonlinearities generate signals similar to a sum of sinusoids with different amplitudes, frequencies, and phases as in the filter proposed by [52].

The next stages of their model [52] consist of the signal threshold and the leaky integrate-and-fire segments. Both parts represent cell membrane properties. The model [52] is restricted to temporal variations of the stimuli but it predicts the time interval of every single spike. Therefore, this model [52] supports our hypothesis that variability in the spike trains expresses intraretinal processes and not exclusively noise.

In the experiment in which the stimulus is spatially restricted to a single G -neuron or to the receptive field of single ganglion cell, the responses show synchronization (with period 1) to the stimulus for most stimulus frequencies and amplitudes (Fig. 9). However, the responses of neighboring G -neurons that are not directly stimulated, show more complicated properties (Fig. 10): They resemble Arnold tongues with many interleaved oscillatory periods as a function of the frequency and amplitude of the input signal. As we have mentioned previously, these different oscillations are related to synchronization of different neuronal subpopulations. Such situation is in Fig. 5(b), where neighboring neurons show different patterns of responses partly synchronized with the stimulus. One interpretation of the results in Fig. 10 is that the stimulated neuron influences the spontaneous activity of neighboring neurons through lateral connections. As a result, the neighboring neurons exhibit complex responses and high sensitivity to the stimulus parameters.

V. CONCLUSION

Neurophysiological experiments [13], [57] and our present model demonstrate that the output (ganglion cell activity) of the retina, the first neural structure in the visual system, may exhibit deterministic patterns of activity with and without input stimuli.

In particular, we propose that spike trains consist of several components.

- 1) One component is related to the local integration of information, in agreement with the center-surround receptive field properties of retinal cells. This component is always locked to the input, like the results of the same calculation repeatedly done on a computer.
- 2) Additional components related to integration of information on several different temporal scales. These components are responsible for synchronization of processes,

potentially extracting different stimulus attributes. They integrate parallel computations by means of synchronized oscillations in different frequency ranges and with different spatial extents. These components may or may not be locked to the input, and, therefore, they may manifest themselves as irregularities in spike trains.

In the lateral geniculate nucleus (LGN), it has been found that activity from the retina is compared [101] with the positive feedback from the cortex [102] and modulated by many other structures [103]. In a theoretical model, we have proposed [104] that the synchronization of neural activity in the retina may be related to formation of the hypothesis about the stimulus. Synchronization in the cortex may form the prediction about the perceived object: Specifically, if the purpose of feedback from cortex is to increase synchronization in LGN, this may be described as checking a complex hypothesis through simple questions.

ACKNOWLEDGMENT

The authors would like to thank M. Kon, P. Kaskan, and M. Rubin for comments. They would also like to thank D. Soldak for conversion of the postscript files from Mac to PC format, and L. Garnett and S. Adham for the editorial help.

REFERENCES

- [1] J. C. Eccles, M. Ito, and J. Szentágothai, *The Cerebellum as a Neuronal Machine*. New York: Springer-Verlag, 1967, pp. 335–335.
- [2] M. A. Arbib, *Brains, Machines, and Mathematics*, 2nd ed. New York: Springer-Verlag, 1988.
- [3] P. S. Churchland and T. J. Sejnowski, *The Computational Brain*. Cambridge, MA: MIT Press, 1992.
- [4] J. R. Searle, “Minds, brains, and programs,” *Behav. Brain Sci.*, vol. 3, pp. 417–457, 1980.
- [5] —, “Is the brain digital computer?,” *Proc. Addresses Amer. Philosophical Assoc.*, vol. 64, pp. 21–37, 1990.
- [6] B. J. Copeland and R. Sylvan, “Beyond the universal Turing machine,” *Australasian J. Philosophy*, vol. 77, pp. 46–67, 1999.
- [7] W. Singer, “Synchronization of cortical activity and its putative role in information processing and learning,” *Ann. Rev. Physiol.*, vol. 55, pp. 349–374, 1993.
- [8] R. Eckhorn, “Cortical synchronization suggests neural principles of visual feature grouping,” *Acta Neurobiol. Exp. (Warsaw)*, vol. 60, pp. 261–9, 2000.
- [9] C. M. Gray and W. Singer, “Stimulus-specific neuronal oscillations in orientation columns of cat visual cortex,” *Proc. Nat. Acad. Sci.*, vol. 86, pp. 1698–702, 1989.
- [10] A. Frien, R. Eckhorn, R. Bauer, T. Woelbern, and H. Kehr, “Stimulus-specific fast oscillations at zero phase between visual areas V1 and V2 of awake monkey,” *NeuroReport*, vol. 5, pp. 2273–2277, 1994.
- [11] L. Wachtmeister and J. E. Dowling, “The oscillatory potentials of the mudpuppy retina,” *Invest. Ophthalmol. Vis. Sci.*, vol. 17, pp. 1176–88, 1978.
- [12] A. W. Przybyszewski, “An analysis of the oscillatory patterns in the central nervous system with the wavelet method,” *J. Neurosci. Methods*, vol. 38, pp. 247–257, 1991.
- [13] A. W. Przybyszewski, M.J.M. Lankheet, and W. A. van de Grind, “Oscillations of the generator potential in X retinal ganglion cells of cat,” *Vis. Res.*, vol. 33, pp. 861–875, 1993.
- [14] H. R. Wilson and J. D. Cowan, “Excitatory and inhibitory interactions in localized populations of model neurons,” *Biophys. J.*, vol. 12, pp. 1–13, 1972.
- [15] B. Baird, “Nonlinear dynamics of pattern formation and pattern recognition in the rabbit olfactory bulb,” *Physica D*, vol. 22, pp. 150–175, 1986.
- [16] W. J. Freeman and K. A. Graski, “Relation of olfactory EEG to behavior: Factor analysis,” *Behav. Neurosci.*, vol. 101, pp. 766–777, 1987.
- [17] M. W. Hirsch and B. Baird, “Computing with dynamic attractors in neural networks,” *Biosyst.*, vol. 34, pp. 173–95, 1995.
- [18] D. G. Aronson, G. B. Ermentrout, and N. Kopell, “Amplitude response of coupled oscillators,” *Physica D*, vol. 41, pp. 403–449, 1990.
- [19] C. Baesens, J. Guckenheimer, S. Kim, and R. S. MacKay, “Three coupled oscillators: Modelocking, global bifurcations and toroidal chaos,” *Physica D*, vol. 49, pp. 387–475, 1991.
- [20] P. S. Lindsay and A. W. Cumming, “Three-frequency quasiperiodicity, phase locking and the onset of chaos,” *Physica D*, vol. 40, pp. 196–217, 1989.
- [21] E. D. Adrian and R. Mathews, “The action of light on the eye. Part III the interaction of retinal neurons,” *J. Physiol.*, vol. 65, pp. 273–298, 1928.
- [22] R. Granit, “Rotation of activity and spontaneous rhythms in retina,” *Acta Physiol. Scandinavia*, vol. 1, pp. 370–379, 1941.
- [23] S. W. Kuffler, “Discharge pattern and functional organization of mammalian retina,” *J. Neurophysiol.*, vol. 16, pp. 37–68, 1953.
- [24] T. E. Ogden, “The oscillatory waves of the primate electroretinogram,” *Vis. Res.*, vol. 13, pp. 1059–74, 1973.
- [25] D. Yonemura and K. Kawasaki, “New approaches to ophthalmic electrodiagnosis by retinal oscillatory potential, drug-induced responses from retinal pigment epithelium and cone potential,” *Doc. Ophthalmol.*, vol. 48, pp. 163–222, 1979.
- [26] M. Ariel, N. W. Daw, and R. K. Rader, “Rhythmicity in rabbit retinal ganglion cell responses,” *Vis. Res.*, vol. 23, pp. 1485–93, 1983.
- [27] H. T. Chung, O.-J. Gruesser, and A. W. Przybyszewski, “An analysis of cat ganglion cells oscillations before and after intravitreal injection of amono-phosphono-butyric acid (APB),” *Soc. Neurosci. Abstract*, vol. 16, pt. 2, pp. 1218–1218, 1990.
- [28] S. Neuenschwander, M. Castelo-Branco, and W. Singer, “Synchronous oscillations in the cat retina,” *Vis. Res.*, vol. 39, pp. 2485–97, 1999.
- [29] A. W. Przybyszewski, P. Guaidino, and N. J. Sucker, “APB modification of spatiotemporal processes in the cat retina: Comparing experiment and simulation,” *Invest. Ophthalmol. Vis. Sci.*, vol. 36, pp. S289–S289, 1995.
- [30] M. Korth, “Luminosity functions of human electroretinogram wavelets evoked with pattern-reversal stimuli,” *Invest. Ophthalmol. Vis. Sci.*, vol. 19, pp. 810–816, 1980.
- [31] —, “Human fast retinal potentials and the spatial properties of a visual stimulus,” *Vis. Res.*, vol. 21, pp. 627–630, 1981.
- [32] H. Heynenn, L. Wachtmeister, and V. D. Norren, “Origin of oscillatory potentials of the retina,” *Vis. Res.*, vol. 10, pp. 1365–1373, 1985.
- [33] L. Wachtmeister, “Basic research and clinical aspects of the oscillatory potentials of the electroretinogram,” *Doc. Ophthalmol.*, vol. 66, pp. 187–194, 1987.
- [34] C. Karwoski and K. Kawasaki, “Oscillatory potentials,” in *Principles and Practice of Clinical Electrophysiology of Vision*, J.R. Heckenlively and G. B. Arden, Eds. St. Louis, MO: Moshby Year Book, 1991, pp. 125–128.
- [35] M. H. Foerster, W. A. van de Grind, and O. J. Grusser, “The response of cat horizontal cells to flicker stimuli of different area, intensity and frequency,” *Exp. Brain Res.*, vol. 29, pp. 367–85, 1977.
- [36] M. J. Lankheet, R. J. Van Wezel, J. H. Prickaerts, and W. A. van de Grind, “The dynamics of light adaptation in cat horizontal cell responses,” *Vis. Res.*, vol. 33, pp. 1153–71, 1993.
- [37] M. J. Lankheet, A. W. Przybyszewski, and W. A. van de Grind, “The lateral spread of light adaptation in cat horizontal cell responses,” *Vis. Res.*, vol. 33, pp. 1173–84, 1993b.
- [38] R. F. Dacheux and E. Raviola, “The rod pathway in the rabbit retina: A depolarizing bipolar and amacrine cell,” *J. Neurosci.*, vol. 6, pp. 331–45, 1986.
- [39] H. M. Sakai and K. Naka, “Dissection of the neuron network in the cat-fish inner retina.V. interactions between NA and NB amacrine cells,” *J. Neurophysiol.*, vol. 63, pp. 120–130, 1990.
- [40] M. I. Veruki and E. Hartveit, “AII (Rod) amacrine cells form a network of electrically coupled interneurons in the mammalian retina,” *Neuron*, vol. 33, pp. 935–46, 2002.
- [41] P. Gaudiano, “Simulations of X and Y retinal ganglion cell behavior with a nonlinear push-pull model of spatiotemporal retinal processing,” *Vis. Res.*, vol. 34, pp. 1767–84, 1994.
- [42] L. Wachtmeister, “On the oscillatory potentials of the human electroretinogram in light and dark adaptation,” *Acta Ophthalmol. Suppl.*, vol. 116, pp. 1–32, 1972.
- [43] —, “Luminosity functions of the oscillatory potentials of the human electroretinogram,” *Acta Ophthalmol. (Copenhagen)*, vol. 52, pp. 353–66, 1974.
- [44] —, “Further studies of the chemical sensitivity of the oscillatory potentials of the electroretinogram (ERG). III. Some omega amino acids and ethanol,” *Acta Ophthalmol. (Copenhagen)*, vol. 59, pp. 609–19, 1981.

- [45] M. H. Munk and S. Neunenschwander, "High-frequency oscillations (20 to 120 Hz) and their role in visual processing," *J. Clinical Neurophysiol.*, vol. 17, pp. 341–60, 2000.
- [46] N. Nakagawa and Y. Kumamoto, "From collective oscillations to collective chaos in a globally coupled oscillator system," *Phys. Rev. D*, vol. 75, pp. 74–80, 1994.
- [47] T. Shibata, T. Chawanya, and K. Kaneko, "Noiseless collective motion out of noisy chaos," *Phys. Rev. Lett.*, vol. 82, pp. 4424–4427, 1999.
- [48] K. Kaneko, "Dominance of milnor attractors and noise-induced selection in a multi-attractor system," *Phys. Rev. Lett.*, vol. 78, pp. 2736–2739, 1997.
- [49] T. Shibata and K. Kaneko, "Collective chaos," *Phys. Rev. Lett.*, vol. 81, pp. 4116–4119, 1998.
- [50] P. Kara, P. Reinagel, and R. C. Reid, "Low response variability in simultaneously recorded retinal, thalamic, and cortical neurons," *Neuron*, vol. 27, pp. 635–46, 2000.
- [51] L. M. Jones, D. A. Depireux, and D. J. Simons, "Keller robust temporal coding in the trigeminal system," *Science*, vol. 304, pp. 1986–9, 2004.
- [52] J. Keat, P. Reinagel, R. C. Reid, and M. Meister, "Predicting every spike: A model for the responses of visual neurons," *Neuron*, vol. 30, pp. 803–817, 2001.
- [53] P. Reinagel and R. C. Reid, "Precise firing events are conserved across neurons," *J. Neurosci.*, vol. 22, pp. 6837–41, 2002.
- [54] J. P. Keener, "Analog circuitry for the van der Pol and FitzHugh-Nagumo equations," *IEEE Trans. Syst. Man., Cybern.*, vol. SMC-13, no. 5, pp. 1010–1015, 1983.
- [55] P. L. Carras, P. A. Coleman, and R. F. Miller, "Site of action potential initiation in amphibian retinal ganglion cells," *J. Neurophysiol.*, vol. 67, pp. 292–304, 1992.
- [56] H. Markram, P. J. Helm, and B. Sakmann, "Dendritic calcium transients evoked by single back-propagating action potentials in rat neocortical pyramidal neurons," *J. Physiol.*, vol. 485, pp. 1–20, 1995.
- [57] A. W. Przybyszewski, M. J. M. Lankheet, and W. A. van de Grind, "On the complex dynamics of intracellular ganglion cell light responses in the cat retina," *Biol. Cybern.*, vol. 74, pp. 299–308, 1996.
- [58] D. N. Mastrorarde, *Correlated Firing of Retinal Ganglion Cells*, vol. 12, pp. 75–80, 1989.
- [59] K. Hartline and F. R. Claff, "Inhibitory interactions of response units in the eye of *Limulus*," *J. Gen. Physiol.*, vol. 40, pp. 1357–1379, 1957.
- [60] G. T. Kenyon and D. W. Marshak, "Gap junctions with amacrine cells provide a feedback pathway for ganglion cells within the retina," *Proc. Royal Soc. London Series B, Biol. Sci.*, vol. 265, pp. 919–25, 1998.
- [61] D. M. Dacey and S. Brace, "A coupled network for parasol but not midget ganglion cells in the primate retina," *Vis. Neurosci.*, vol. 9, pp. 279–290, 1992.
- [62] E. J. Chichilnisky and D. A. Baylor, "Synchronized firing by ganglion cells in monkey retina," *Soc. Neurosci. Abstract*, vol. 25, pp. 1042–1042, 1999.
- [63] D. N. Mastrorarde, "Correlated firing of cat retinal ganglion cells. I. spontaneously active inputs to X- and Y-cells," *J. Neurophysiol.*, vol. 49, pp. 303–324, 1983.
- [64] —, "Correlated firing of cat retinal ganglion cells. II. Responses of X- and Y-cells to single quantal events," *J. Neurophysiol.*, vol. 49, pp. 325–349, 1983.
- [65] —, "Interactions between ganglion cells in cat retina," *J. Neurophysiol.*, vol. 49, pp. 350–365, 1983c.
- [66] S. H. DeVries, "Correlated firing in rabbit retinal ganglion cells," *J. Neurophysiol.*, vol. 81, pp. 908–920, 1999.
- [67] I. H. Brivanlou, D. K. Warland, and M. Meister, "Mechanisms of concerted firing among retinal ganglion cells," *Neuron*, vol. 20, pp. 527–539, 1998.
- [68] M. Meister, L. Vanado, and D. A. Baylor, "Concerted signaling by retinal ganglion cells," *Science*, vol. 270, pp. 1207–10, 1995.
- [69] E. H. Hu and S. A. Bloomfield, "Gap junctional coupling underlies the short-latency spike synchrony of retinal alpha ganglion cells," *J. Neurosci.*, vol. 23, no. 17, pp. 6768–77, Jul. 2003.
- [70] S. Hidaka, Y. Akahori, and Y. Kurosawa, "Dendrodendritic electrical synapses between mammalian retinal ganglion cells," *J. Neurosci.*, vol. 24, no. 46, pp. 10553–67, Nov. 2004.
- [71] T. Schubert, J. Degen, K. Willecke, S. G. Hormuzdi, H. Monyer, and R. Weiler, "Connexin36 mediates gap junctional coupling of alpha-ganglion cells in mouse retina," *J. Comparative Neurol.*, vol. 485, pp. 191–201, 2005.
- [72] B. Volgyi, J. Abrams, D. L. Paul, and S. A. Bloomfield, "Morphology and tracer coupling pattern of alpha ganglion cells in the mouse retina," *J. Comparative Neurol.*, vol. 492, pp. 66–77, 2005.
- [73] R. W. Rodieck, "Maintained activity of cat retinal ganglion cells," *J. Neurophysiol.*, vol. 30, pp. 1043–1071, 1967.
- [74] T. Sato, M. Yamamoto, and H. H. Nakahama, "Variability of interspike intervals of cat's on-center optic tract fibres activated by steady light spot: A comparative study on X- and Y-fibres," *Exp. Brain Res.*, vol. 24, pp. 285–93, 1976.
- [75] M. W. Levine, "The distribution of the intervals between neural impulses in the maintained discharges of retinal ganglion cells," *Biol. Cybern.*, vol. 65, pp. 459–467, 1991.
- [76] H. B. Barlow and W. R. Levick, "Changes in the maintained discharge with adaptation level in the cat retina," *J. Physiol.*, vol. 202, no. 3, pp. 699–718, Jun. 1969.
- [77] L. J. Frishman and M. W. Levine, "Statistics of the maintained discharge of cat retinal ganglion cells," *J. Physiol.*, vol. 339, pp. 475–494, 1983.
- [78] W. Kuffler, R. FitzHugh, and H. B. Barlow, "Maintained activity in the cats retina in light and darkness," *J. Gen. Physiol.*, vol. 40, pp. 295–316, 1957.
- [79] M. W. Levine and R. P. Zimmerman, "A model of the variability of maintained discharges and responses to flashes of light," *Biol. Cybern.*, vol. 65, pp. 469–477, 1991.
- [80] N. Takahashi, Y. Hanyu, T. Musha, R. Kubo, and G. Matsumoto, "Global bifurcation structure in periodically stimulated giant axons of squid," *Physica D*, vol. 43, pp. 318–334, 1990.
- [81] A. Cumming and P. S. Linsay, "Quasiperiodicity and chaos in a system with three competing frequencies," *Phys. Rev. Lett.*, vol. 60, pp. 2719–2722, 1988.
- [82] P. Linsay and A. Brailove, "Experiments with coupled nonlinear oscillators," in *Proc. 1st Exp. Chaos Conf.*, Arlington, VA, Oct. 1–3, 1991–1992, pp. 34–49.
- [83] D. P. Lathrop and E. J. Kostelich, "Characterization of an experimental strange attractors by periodic orbits," *Phys. Rev. A*, vol. 40, pp. 4028–40, 1989.
- [84] M. J. Schnitzer and M. Meister, "Multineuronal firing patterns in the signal from eye to brain," *Neuron*, vol. 37, pp. 499–511, 2003.
- [85] M. W. Levine, "Variability of maintained discharges of retinal ganglion cells," *J. Optical Soc. Amer.*, vol. A 4, pp. 2308–20, 1987.
- [86] —, "Modeling the variability of firing rate of retinal ganglion cells," *Math Biosci.*, vol. 112, pp. 225–42, 1992.
- [87] M. J. Lankheet, J. Molenaar, and W. A. van de Grind, "The spike generating mechanism of cat retinal ganglion cells," *Vis. Res.*, vol. 29, pp. 505–17, 1989.
- [88] R. FitzHugh, "Impulses and physiological states in models of nerve membrane," *Biophys. J.*, vol. 1, pp. 445–466, 1961.
- [89] J. A. Glazier and A. Libchaber, "Quasi-periodicity and dynamical systems: An experimentalists view," *IEEE Trans. Circuits Syst.*, vol. 35, no. 7, pp. 790–809, Jul. 1988.
- [90] G. B. Ermentrout and N. Kopell, "Fine structure of neural spiking and synchronization in the presence of conduction delays," *Proc. Nat. Acad. Sci.*, vol. 95, pp. 1259–64, 1998.
- [91] A. W. Przybyszewski, M. J. M. Lankheet, and W. A. van de Grind, W. Dito, L. Pecora, S. Vohra, M. Shlesinger, and M. Spano, Eds., "Irregularities in spike train of cat retinal ganglion cells," in *Proc. 2nd Conf. Exp. Chaos*, 1995, pp. 218–225.
- [92] M. W. Levine, "Retinal processing of intrinsic and extrinsic noise," *J. Neurophysiol.*, vol. 48, pp. 993–1008, 1982.
- [93] M. C. Teich, C. Heneghan, S. B. Lowen, T. Ozaki, and E. Kaplan, "Fractal character of the neural spike train in the visual system of the cat," *J. Opt. Soc. Amer.*, vol. 14, pp. 529–46, 1997.
- [94] S. B. Lowen, T. Ozaki, E. Kaplan, B. E. Saleh, and M. C. Teich, "Fractal features of dark, maintained, and driven neural discharges in the cat visual system," *Methods*, vol. 24, pp. 377–94, 2001.
- [95] M. N. Shadlen and W. T. Newsome, "Noise, neural codes and cortical organization," *Current Opinion Neurobiol.*, vol. 4, pp. 569–79, 1994.
- [96] A. Grinvald, A. Arieli, M. Tsodyks, and T. Kenet, "Neuronal assemblies: Single cortical neurons are obedient members of a huge orchestra," *Biopolymers*, vol. 68, pp. 422–36, 2003.
- [97] T. Kenet, D. Bibitchkov, M. Tsodyks, A. Grinvald, and A. Arieli, "Spontaneously emerging cortical representations of visual attributes," *Nature*, vol. 425, pp. 954–6, 2003.
- [98] J. Schummers, J. Marino, and M. Sur, "Synaptic integration by V1 neurons depends on location within the orientation map," *Neuron*, vol. 36, pp. 969–78, 2002.
- [99] M. Tsodyks, T. Kenet, A. Grinvald, and A. Arieli, "Linking spontaneous activity of single cortical," *Neurons Underlying Functional Architecture Sci.*, vol. 286, pp. 1943–6, 1999.

- [100] A. Arieli, A. Sterkin, A. Grinvald, and A. Aertsen, "Dynamics of ongoing activity: Explanation of the large variability in evoked cortical responses," *Science*, vol. 273, pp. 1868–71, 1996.
- [101] L. Maffei and A. Fiorentini, "Retinogeniculate convergence and analysis of contrast," *J. Neurophysiol.*, vol. 35, pp. 65–72, 1972.
- [102] A. W. Przybyszewski, J. G. Gaska, W. Foote, and D. A. Pollen, "Striate cortex increases contrast gain of macaque LGN neurons," *Vis. Neurosci.*, vol. 17, pp. 485–494, 2000.
- [103] S. M. Sherman and R. W. Guillery, "The role of the thalamus in the flow of information to the cortex," *Philosoph. Trans. Royal Soc. London Ser. B, Biol. Sci.*, vol. 357, pp. 1695–708, 2002.
- [104] A. W. Przybyszewski and M. A. Kon, Synchronization Based Model of the Visual System Supports Cognition Soc. Neurosci., Washington, DC, 2003, Program No. 718.11. 2003 Abstract Viewer/Itinerary Planner.
- [105] E. M. Izhikevich, "Which model to use for cortical spiking neurons?," *IEEE Trans. Neural Netw.*, vol. 15, no. 5, pp. 1063–70, Sep. 2004.
- [106] D. Xu and J. C. Principe, "Dynamical analysis of neural oscillators in an olfactory cortex model," *IEEE Trans. Neural Netw.*, vol. 15, no. 5, pp. 1053–62, Sep. 2004.
- [107] R. Eckhorn, A. M. Gail, A. Bruns, A. Gabriel, B. Al-Shaikhli, and M. Saam, "Different types of signal coupling in the visual cortex related to neural mechanisms of associative processing and perception," *IEEE Trans. Neural Netw.*, vol. 15, no. 5, pp. 1039–52, Sep. 2004.
- [108] G.T. Kenyon, J. Theiler, J. S. George, B. J. Travis, and D. W. Marshak, "Stimulus-specific oscillations in a retinal model," *IEEE Trans. Neural Netw.*, vol. 15, no. 5, pp. 1083–91, Sep. 2004.



Andrzej W. Przybyszewski received the M.S. degree in electrical engineering from Warsaw Polytechnic, Warsaw, Poland, the M.A. degree in mathematics from Warsaw University, Warsaw, Poland, and the Ph.D. degree in neurophysiology from Warsaw Medical Academy, Warsaw, Poland.

He is an Assistant Professor of Neurology at the University of Massachusetts, Worcester, and is currently a visiting Professor at the Department of Psychology, McGill University, Montreal, Canada. The long term goal of his research is to understand

how the brain integrates streams of the sensory information and converts them into the action. He has performed recordings from the retina while he was working with O.-J. Grusser in Berlin, Germany, and with W. van de Grind and M. Lankheed in Utrecht, The Netherlands. Later with D. Pollen (University of Massachusetts) and M. Snodderly and I. Kagan (Schepens Institute, Harvard Medical School, Cambridge, MA), he has performed recordings from LGN, V1, and V4 areas in monkeys. Backprojecting (feedback) pathways play a major role in brain function (work with D. Pollen, and anatomy analysis with K. Rockland during his stay at the RIKEN Institute, Saitama, Japan). Currently, he is studying behavior of marmoset monkeys (*Behavioral Brain Research*, 2006) and he is preparing wireless recording system to record from the visual system in freely moving marmosets. These data are being modeled in cooperation with M. Kon (Boston University, Boston, MA) and T. Rutkowski (RIKEN). The

main stream of his work follows the idea of P. Ricoeur described in his book *Soi-même comme un autre* (Seuil: Paris, France, 1990) that an individual's identity has its base not only in genes but also in individual actions which fingerprints the way that parallel processes are integrated in the brain.

Paul S. Linsay received the Ph.D. degree in experimental physics from the University of Chicago, Chicago, IL, in 1977.

From 1979 to 1997, he was a Principal Research Scientist at the Department of Physics, Massachusetts Institute of Technology (MIT), Cambridge. In 1999, he was a Senior Member of the Technical Staff at Motorola. Since 1997, he has been a Principal of Linsay Associates, Newton, MA, providing scientific solutions to industrial problems.



Paolo Gaudiano received the B.S. degree in applied mathematics and the M.S. degree in aerospace engineering from the University of Colorado, Boulder, in 1984 and 1987, respectively, and the Ph.D. degree in cognitive and neural systems from Boston University, Boston, MA.

In late 2001, he joined Icosystem Corporation, Cambridge, MA, as a Chief Technology Officer, where he oversees research and development efforts across a broad spectrum of technical and business areas, focusing on consumer behavior, predictive modeling and optimization. He began his career as a Faculty Member at Boston University, Boston, MA, where he specialized in applied research in neural networks and robotics. In 1998, he became a Chief Scientist at Artificial Life, Inc., a company that applied natural language processing and autonomous agent technology to a variety of Internet usage and navigation problems.

Dr. Gaudiano is the recipient of several awards, including a Young Investigator Award from the Office of Naval Research and a Sloan Fellowship in Neuroscience.



Christopher M. Wilson received the B.S. degree in physics from the Massachusetts Institute of Technology (MIT), Cambridge, in 1996, where he performed undergraduate research on the role of nonlinear dynamics in the nervous system. He received the Ph.D. degree in physics from Yale University in 2002. His dissertation focused on the development of single-photon spectrometers using superconducting tunnel junctions.

He then worked at Yale as the W.M. Keck Postdoctoral Fellow performing research on quantum computation and information processing using superconducting single electronics. Since 2004, he has been with Chalmers University of Technology, Goetheborg, Sweden, where he continues work on quantum computation.